

Functional and Morphological Organization of the Rabbit Sinus Node

WIM K. BLEEKER, ALBERT J.C. MACKAAY, MIREILLE MASSON-PÉVET,
LENNART N. BOUMAN, AND ANTON E. BECKER

SUMMARY In isolated right atria of the rabbit heart, we studied the activation pattern within the sinus node, using the microelectrode technique. After the electrophysiological experiments, the preparations were subjected to a correlative morphological investigation, using light or electron microscopy. Different criteria for defining the dominant pacemaker were compared. A group of at least 5000 cells, located within the central part of the node where the most characteristic tissue architecture was found, was considered to be responsible for generation of the impulse. At the ultrastructural level, this leading cell group appeared to be part of a larger uniform cell group. The number of gap junctions observed suggests that all nodal cells are coupled by these structures. Toward the periphery, the excitation wave was propagated preferentially in an oblique cranial direction toward the crista terminalis. Neither morphologically nor electrophysiologically specific pathways were found for the conduction, but the preferential direction could be explained by the tissue architecture. *Circ Res*: 46: 11-22, 1980

ELECTROPHYSIOLOGICAL studies have revealed that, in the rabbit sinus node, only a small group of cells generates the impulse and that the major part consists of cells with pacemaker characteristics which, however, normally serve only as a conductor of the excitation wave (for review, see: Brooks and Lu, 1972). Histological studies have shown the rabbit sinus node to be a rather large structure (James, 1967; Truex, 1976), which is not homogeneous at ultrastructural level (for recent review of the ultrastructure, see Tranum-Jensen, 1976). From the Morphology, it is not possible to predict the precise location of the pacemaker (James, 1967). For electrophysiological location of the dominant pacemaker, several criteria have been mentioned in the literature: (1) earliest activation (West, 1955; Paes de Carvalho, 1961; Sano and Yamagishi, 1965); (2) fast diastolic depolarization (e.g., West, 1955; Paes de Carvalho, 1961); (3) slow phase 0 depolarization (Kohlhardt, 1976; Seyama, 1976); and (4) gradual transition from diastolic into systolic depolarization (e.g., Paes de Carvalho, 1961; Trautwein and Uchizono, 1963). To locate the dominant pacemaker as precisely as possible, we compared these criteria and tried to evaluate their relationship. In addition, we performed a histological study of preparations of which the site of origin and the conduction paths of the impulse had been mapped previously. To determine in which part of the sinus node the electrophysiologically identified pacemaker was located, the histological reconstruc-

tion was correlated with the activation map. Furthermore, we attempted to find a morphological basis for the conduction pattern toward the periphery, as was described by Sano and Yamagishi (1965).

Another question in this study was how the communication between nodal cells, which is needed for synchronization and conduction, is effected. The numerous electron microscopic studies dealing with the sinus node conspicuously give no answer to this. Trautwein and Uchizono (1963), who investigated the ultrastructure of electrophysiologically identified dominant and latent pacemaker cells, did not describe the intercellular junctions. Other authors, who performed their studies without prior electrophysiological identification, reported that gap junctions (nexuses), which are generally accepted to be responsible for electrical coupling in other cardiac tissues, were exceedingly rare (Tranum-Jensen, 1976, rabbit) or even absent (James et al., 1966, man and dog; Ayettey and Navaratnam, 1978, rat). This observation was even a basis for a hypothesis that intercellular communication in the sinus node occurs not electrically but mechanically by stretch (Pollack, 1977). Since evidence for electrical coupling can be found in the studies of the passive electrical properties of the sinus node (Bonke, 1973; Seyama, 1976; Bukauskas et al., 1977), we judged it worthwhile to perform another electron microscopic study of electrophysiologically identified samples from the sinus node, paying special attention to the intercellular junctions.

Methods

Preparation

Rabbits (2.5–3 kg) of both sexes were anesthetized with either Nembutal (Na pentobarbital, 20 mg/kg, iv) + ether inhalation or Hypnorm (10 mg

From the Department of Physiology, University of Amsterdam and the Department of Pathology, Wilhelmina Gasthuis, Amsterdam, The Netherlands.

Dr. Becker is affiliated with the Department of Pathology, Wilhelmina Gasthuis, Amsterdam, The Netherlands.

Address for reprints: Dr. L.N. Bouman, Department of Physiology, University of Amsterdam, Eerste Const. Huygensstraat 20, 1054 BW Amsterdam, The Netherlands.

Received June 16, 1978; accepted for publication September 4, 1979.

of fluanison + 0.2 mg of fentanyl base per kg, im). The heart was excised rapidly and immersed in an oxygenated balanced salt solution. The preparation, including the sinus node, the intercalvical region, and the roof of the right atrial appendage, but not the atrioventricular node and the interatrial septum, was mounted on a perforated silicon rubber block in a tissue bath, exposing the endocardial surface. The upper part of the crista terminalis was cut to obtain a good exposure of the sinus node. The bathing solution was modified after McEwen (1956): NaCl, 130.6 mM; NaHCO₃, 24.2 mM; KCl, 5.6 mM; CaCl₂, 2.2 mM; MgCl, 0.6 mM; glucose, 11.1 mM; saccharose, 13.2 mM; saturated with a mixture of 95% O₂ and 5% CO₂, pH 7.4, and perfused the 5-ml tissue bath at a rate of 20 ml/minute. Temperature was kept constant within 0.1° at 38°C.

Recording of Electrical Activity

Transmembrane potentials were recorded by means of the conventional glass microelectrode technique. The microelectrode was mounted in a micromanipulator on a mechanical stage, the lateral movements of which were read with vernier scales accurate to 0.01 mm (Schreurs et al., 1974). The two-dimensional coordinates of each impaled cell were noted. A unipolar surface electrode, placed on the inferior part of the crista terminalis, provided a simple biphasic electrogram (Masuda and Paes de Carvalho, 1975), which was used as a time reference. The beat-to-beat interval was recorded continuously.

Mapping of the Propagation of Excitation

A map of the propagation of excitation was made using the recordings of transmembrane potential of a great number of cells. As the activation moment of a cell, we chose the moment that the voltage was halfway between the maximal diastolic potential and the top of the action potential (V_{hfamp}). A provisional map was made during the experiment. The activation moment of the impaled cells was estimated on an oscilloscope and timed with respect to the reference by means of a digital interval counter. The values obtained were plotted directly on a grid according to the coordinates of the impaled site. Mapping was refined where propagation was found to be slow (e.g., in the pacemaker region). Within 3–5 hours, we impaled with one microelectrode 150–300 cells in an area of about 4 by 6 mm. In the pacemaker region, the distance between two impalements was 0.2 mm. In this way, an activation map was made in 25 preparations. Four preparations in which the impulse was generated by an ectopic focus in the crista terminalis were excluded from the series. In 10 preparations that were intended for electron microscopic study, mapping was confined mainly to the pacemaker region to minimize the morphological deterioration due to long experimentation.

Data Processing

All recorded electrical signals were stored on magnetic tape. Data to produce the final accurate map were obtained from off-line computer analysis. For each impaled cell, the action potential and the atrial surface electrogram were sampled at 1-msec intervals during four consecutive beats. After smoothing and averaging, several parameters of the action potential could be calculated. The time interval between the moment of V_{hfamp} and the steepest deflection of the surface electrogram was measured with an accuracy of ± 1 msec. The activation times of the cells were calculated with respect to the cell that appeared to discharge earliest in the cycle. After plotting these values, isochrones were drawn.

Light Microscopy

To be able to correlate the histological findings with the electrophysiological data, several points of the coordinate system of the activation map were marked on the preparation after the electrical recording was finished. For this, we filled the microelectrode with a 1% solution of Alcian Blue (Lee et al., 1969) and made dots (diameter, 50–100 μm) iontophoretically on the endocardial surface. The coordinate system was marked with 10–15 dots and, in addition, some electrophysiologically important sites were marked (e.g., the pacemaker site).

After completion of the electrophysiological experiment, the preparation, still mounted to the silicon rubber block, was fixed in buffered formalin and dehydrated. To obtain a reference for measurements in the sections, we trimmed the septal edge of the preparation to a straight line after fixation. After removing the rubber block, the preparation was embedded in paraffin wax and serially sectioned (thickness, 7 μm) perpendicular to the crista terminalis. In addition, one preparation was sectioned in a plane parallel to the endocardial surface. Every 10th section was stained with an elastic tissue stain and counterstained according to Van Gieson (Lawson, 1936). After location of the blue dots in the sections, it was possible to determine the place of the section and the actual direction of sectioning with respect to the coordinate system; furthermore, the amount of shrinkage of the preparation, caused by fixation and embedding, could be approximated. The distance of histological structures to the trimmed edge of the preparation was measured by means of an ocular micrometer. Thus we were able to project these structures onto the grid of the activation map. A two-dimensional reconstruction of the morphology of the sinus node was made.

Electron Microscopy

In 10 preparations, several sites were marked with Alcian Blue after completion of the electrophysiological mapping for examination in the electron microscope.

The preparation, still mounted to the silicon rubber block, was immersed in cold 2% paraformaldehyde and 2.5% glutaraldehyde in 0.1 M cacodylate buffer, pH 7.4 (Karnowsky, 1967), for one night. Afterward the preparation was washed in 0.2 M cacodylate buffer, pH 7.4, and at the selected sites, blocks of 0.05–0.08 × 0.2 mm, parallel to the crista terminalis, were cut out. The small tissue blocks obtained were then postfixed in 1% OsO₄ in 0.2 M phosphate buffer, pH 7.4, during 1 hour at 4°C, washed again in 0.2 M cacodylate buffer, pH 7.4, immersed in 0.5% magnesium uranyl acetate in 0.9% NaCl at room temperature during 20 minutes, and embedded in Araldite (Glauert and Glauert, 1958). The sections were cut on a Reichert ultramicrotome with a glass or diamond knife and stained with lead citrate (Reynolds, 1963).

Results

The findings of this study will be presented in the following order. First, an overall view will be given of the electrophysiological and morphological mapping experiments; thereafter, details will be given of the pacemaker area and the peripheral zones of the node. Although there was a distinct variability between the preparations, the described experiments can be regarded as representative.

Mapping of the Nodal Area: Activation Pattern and Histological Reconstruction

In 11 preparations, we explored with a microelectrode an area of about 4 by 6 mm. The spread of excitation showed a similar pattern in all experiments (Fig. 1a), which was in accordance with the results obtained by Paes de Carvalho (1961) and by Sano and Yamagishi (1965). The site of earliest discharge was located in the intercalvular region, 0.5–2 mm away from the medial border of the crista terminalis. From this site, the excitation wave propagated preferentially in an oblique cranial direction toward the crista terminalis. In all other directions, the spread of excitation was markedly slower, and conduction was blocked toward the interatrial septum. Whether this block was partial or complete could not be detected, because the excitation wave reached the septal side of the preparation by circumventing the zone of block both superiorly and inferiorly. In the blocking area, double-component action potentials were recorded, so that it seemed meaningless to determine one activation moment in this zone (see also Fig. 8).

In six of the 11 preparations in which electrophysiological mapping was performed, a morphological reconstruction of the nodal area was obtained and correlated with the activation map (Fig. 1, b and c). The sinus node was identified in the intercalvular region as a large group of cells (yellow in Fig. 1, b and c), which differed from the atrial cells by their staining properties. A head and tail part

could be recognized. Within the nodal cell group, different architectural zones were discriminated. In the central portion of the head of the node, a compact arrangement of interweaving cells embedded in a network of collagen fibers was present (Fig. 1b, inset II). This architecture is indicated in the diagrams of Figure 1 by black dots; it continued into the tail part of the node, although the interweaving arrangement of the cells became less prominent. With respect to the distance to the medial border of the crista terminalis, there was a correlation between the site of the compact portion of the node and the earliest discharging cell group. The central compact part of the node was surrounded by cells that showed a different architectural arrangement. Instead of a compact interweaving structure, the cells now presented themselves in a more or less parallel fashion (Fig. 1b, inset I). This peripheral zone of the node was broad toward the crista terminalis, whereas a small fringe bordered upon the side of the atrial septum.

Pacemaker Area

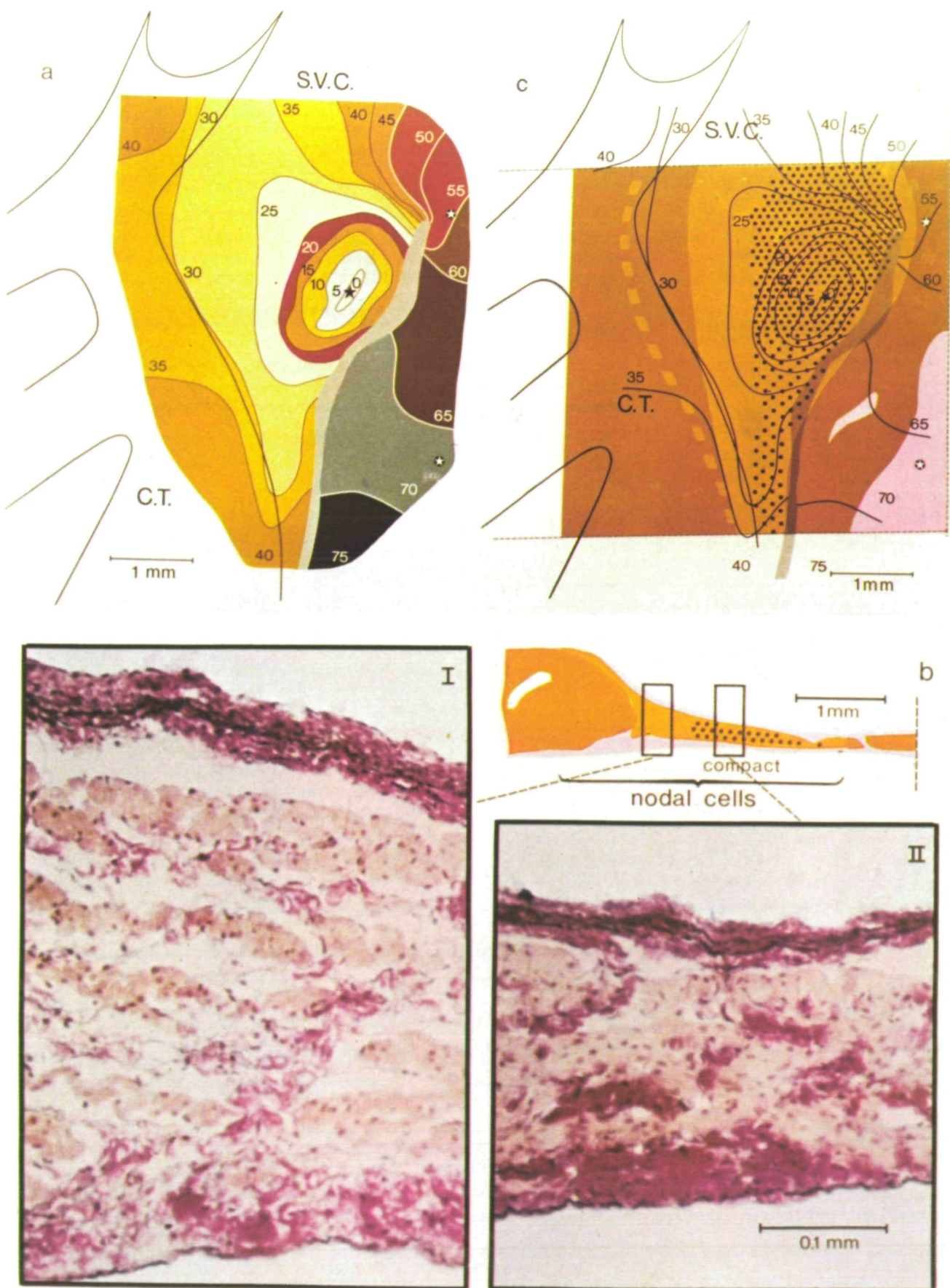
We mapped several electrophysiological characteristics of pacemaker cells, as mentioned in the literature, and correlated them with the morphology.

Earliest Activation Moment

Cells that reached V_{hfamp} earliest were identified in the activation map (Fig. 1a); cells that had this feature in common covered an area of about 0.1 mm². Because V_{hfamp} is an arbitrarily chosen point in the action potential, as an approximation of the excitation threshold, we also timed the moments of steepest rise of the action potentials (\dot{V}_{max}), as was done by Sano and Yamagishi (1965). The cells that reached \dot{V}_{max} earliest were situated closer to the crista terminalis (0.2–0.6 mm, see Fig. 4). In all reconstructed preparations, both the cells that reached V_{hfamp} earliest and the cells that reached \dot{V}_{max} earliest lay within the compact head of the node.

The Lowest Rate of Phase 0 Depolarization (Kohlhardt et al., 1976; Seyama, 1976)

Figure 2 shows a three-dimensional plot of \dot{V}_{max} values (represented by the oblique bars) made on the grid of the activation map. It shows a rather large area with very low values of \dot{V}_{max} . Comparison with the activation map (Figs. 2, 1a) shows that low values of \dot{V}_{max} correspond with a low conduction velocity (2–8 cm/sec) and that the area with very low values of \dot{V}_{max} (see also Fig. 4) includes early as well as late activated cells. Comparing this plot with the morphological reconstruction (Figs. 2 and 1b), one can see that the whole compact part of the node corresponds with the area with low values of \dot{V}_{max} ; values higher than 10 V/sec were measured only in the tail part.



*The Highest Rate of Diastolic Depolarization
(Paes de Carvalho, 1961)*

Because the course of diastolic depolarization is not linear, we measured its rate for all impaled cells at corresponding moments in the cardiac cycle. Figure 3 gives plots of the values of dV/dt (represented by the vertical bars), measured at four arbitrarily chosen moments during the transition from diastolic to phase 0 depolarization. In the first two plots, the highest rates are found in an area of about 0.3 mm^2 (shaded in Figs. 3 and 4), which was situated within the compact portion of the node (Fig. 4). Although within the small area the evolution of the diastolic depolarization was almost identical, small differences in timing and course of the action potentials were observed, as is shown in Figure 4. Identical and synchronous electrical activity was found only in a centrally located area of about 0.1 mm^2 (indicated by a black star). In this area, V_{hfamp} was reached earliest also.

For electron microscopic examination of leading pacemaker cells, we selected in six preparations small pieces of tissue from the center of the area where the highest rate of diastolic depolarization was found. Figure 5 shows a typical example of the ultrastructure of cells from this area. The cardiac cells were of one type only. They were roughly spindle-shaped with a maximum length of $25\text{--}30 \mu\text{m}$, an irregular profile in cross-section, and a diameter smaller than $8 \mu\text{m}$. The long axis was roughly parallel to the crista terminalis. These cells contained a relatively large nucleus and few myofilaments which were found free in the cytoplasm or bundled in myofibrils, loosely organized, with thick irregular Z-lines. The structures present in these cells and particularly the myofibrils were organized much less axially than in atrial cells, whereas the volume occupied by mitochondria and sarcoplasmic reticulum seemed to be less. In contrast, caveolar invaginations were present in a larger number in pacemaker cells, and glycogen granules abounded. The extracellular space was widened

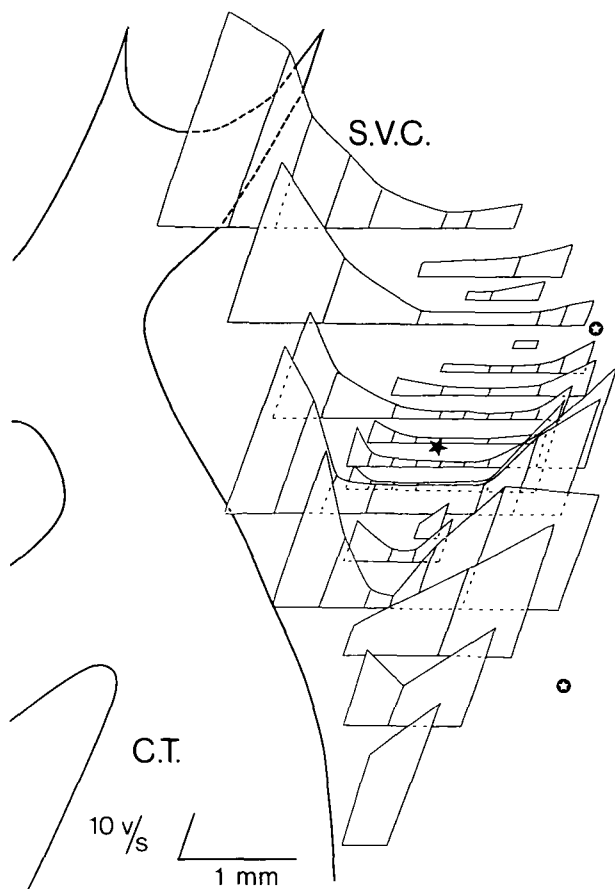


FIGURE 2 *Spatial distribution of V_{max} within the sinus node. The oblique bars indicate the values of \dot{V}_{max} (V/sec). The plot is made on the grid of the activation map of Figure 1, which concerns the same preparation. Action potentials from imperfect impalements were not used.*

compared with that observed in control experiments, without prior electrophysiological study, in which most of the cells were found in close apposition (about 20 nm apart).

FIGURE 1 *a: Map of the activation pattern within the sinus node as seen from the endocardial surface. The activation times are grouped in classes of 5 msec. The light grey (hatched) area indicates the zone in which action potentials with double components were observed. The black and white stars are intended for easier comparison of this figure with Figures 2 and 4, which describe the same preparation. CT = crista terminalis; SVC = superior vena cava. b: Light microscopy of the intercaval region. Same preparation as in a. The right panel shows a schematic reproduction of a section through the sinus node perpendicular to the crista terminalis, at the level of the site of earliest discharge (black star in a). This section shows, at the left side, the thick muscle mass of the crista terminalis. The interatrial septum lies at the right side but is outside the reconstructed area. The endocardial side is upward. Brown = atrial cells; yellow = nodal cells, which partly overlie the crista terminalis; violet = no myocardial cells, only connective tissue. At the level of the black dots, a compact arrangement of interweaving cells was observed, as can be seen at higher magnification in inset II. In the surrounding part of the node, the cells were arranged more regularly, as can be seen in inset I (all cells in cross-section). The enlargement of the intercellular space was more pronounced here than in the interweaving part of the node; in a control experiment, without prior electrophysiological study, enlargement of the extracellular space was not observed. c: Two-dimensional reconstruction of the histology projected on the activation map. Yellow = nodal cells; the nodal cell group has a broad upper part (head) and a tapering end (tail); it partly overlies the crista terminalis. Brown = atrial cells; violet = no myocardial cells, only connective tissue. The black dots indicate the interweaving tissue architecture. The hatched area in the activation map indicates the zone with double-component action potentials (same as the light grey zone in a).*

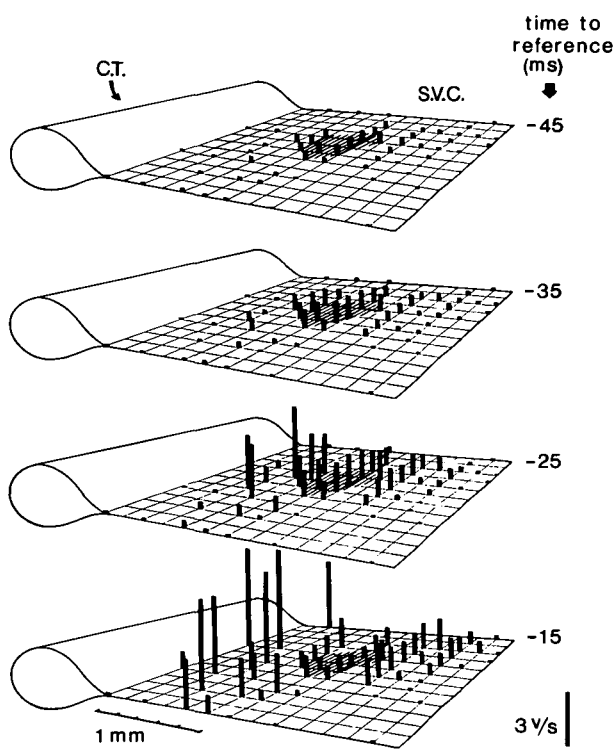


FIGURE 3 Evolution of dV/dt of transmembrane records during the transition from slow diastolic depolarization to nodal firing: spatial distribution of dV/dt values at four moments around the end of diastole. The time interval to the surface electrogram is indicated on the right of each plot (in msec). The vertical bars indicate the instantaneous rate of depolarization (V/sec). The grid represents a small part of the same preparation as was used for Figures 1, 2, and 4. The area with the highest values at -45 and -35 msec is shaded; this area corresponds to the striped area in Figure 4. Action potentials from imperfect impalements were not used.

The specialized junctions, currently described for myocardial tissue, were all present between these nodal cells: fasciae adherentes, desmosomes, and gap junctions. Gap junctions were certainly fewer in number and smaller in size than those between atrial cells, but at least one gap junction was found along every cell contour, as seen in ultrathin sections. They were present at random and not in preferential zones, as between atrial cells, where they can be found in the intercalated discs. Until about 0.5 mm away from this site (in all directions), cells did not reveal any obvious difference from this cell type. We never observed the so called "intercalated clear cells" (Tranum-Jensen, 1976) or "large P-cells" (Truex, 1976), characterized by being larger and paler than the type described above, which are found by several authors to occur singly in the node.

Peripheral Zones

A conspicuous aspect of the spread of excitation toward the periphery is the preference of the con-

duction in the direction of the crista terminalis. In this direction, the conduction velocity increased markedly as soon as the activation front left the compact portion of the node (Fig. 1c). The fastest conduction (20–80 cm/sec) was in the direction of the long axis of the nodal cells, which are arranged here roughly parallel to the crista terminalis. The activation front simultaneously reached a broad part of the crista terminalis. Tissue continuity was

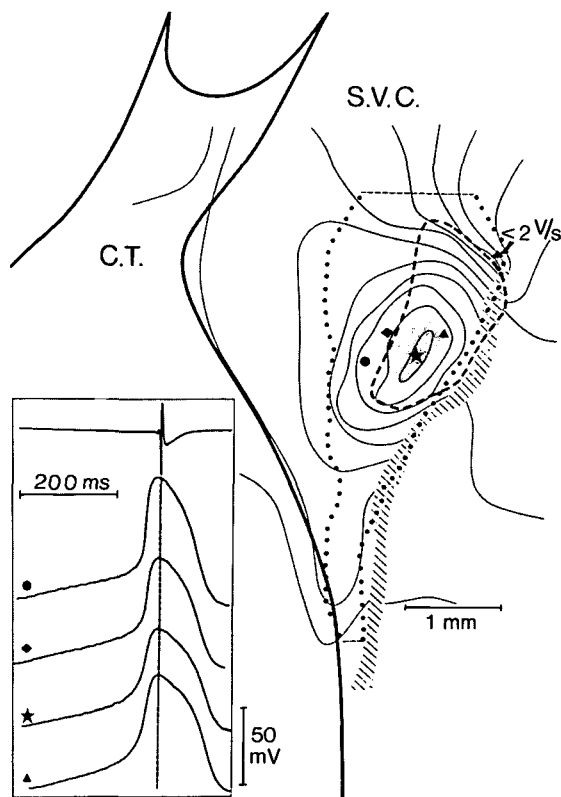


FIGURE 4 Correlation of some electrophysiological characteristics of pacemaker cells and the histological reconstruction. The interrupted line encloses the area with \dot{V}_{max} values of less than 2 V/sec (1.2–2 V/sec). Within the shaded area (same as shaded area in Fig. 3), the fastest evolution of diastolic depolarization was measured. The black star in the center of this area indicates a small area of about 0.1 mm^2 in which synchronous and identical electrical activity was recorded; at the same site, V_{hfamp} was reached earliest. \dot{V}_{max} was observed earliest in a small area, indicated by the black dot. The inset shows transmembrane potentials, recorded at sites with corresponding symbols. It can be seen that early in diastole all four records have the same steepness; an acceleration of depolarization can be observed earliest in the record marked with a black star. Furthermore, it shows clearly the differences in upstroke velocity, amplitude, and duration of the action potentials. All three traced areas lay within the central part of the node that was characterized by a compact interweaving tissue architecture (enclosed by the dotted line, compare with Fig. 1C).

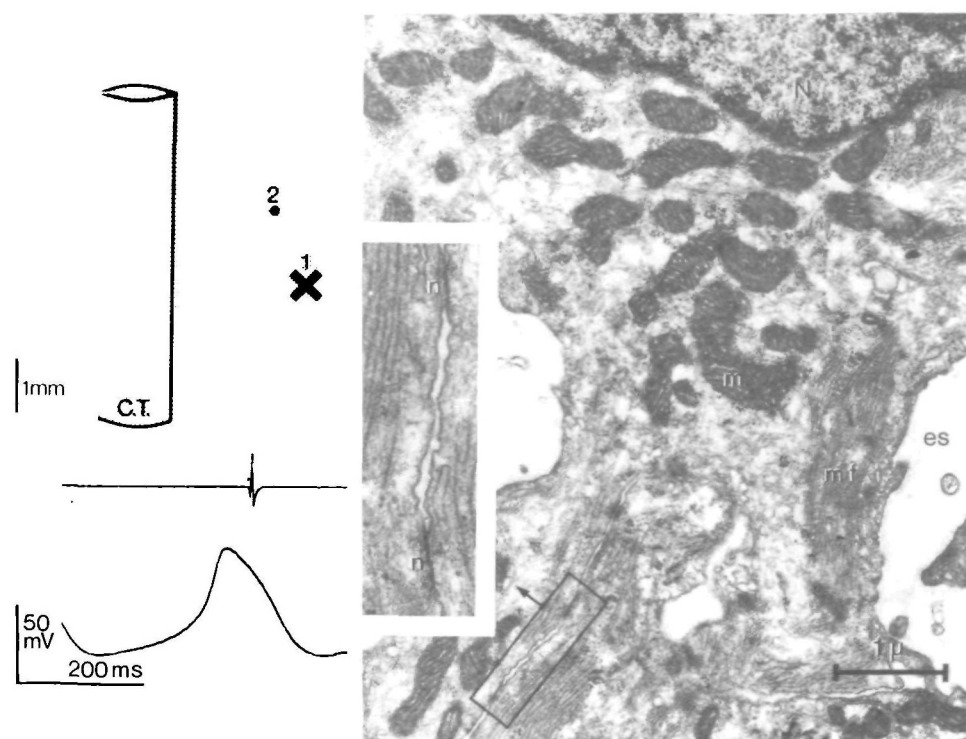


FIGURE 5 Ultrastructure of cells which reached V_{hamp} the earliest and had the fastest diastolic depolarization. On the left, a scheme which shows the location of these cells (site 1) related to the crista terminalis. Underneath, an action potential recorded at this site, together with the surface electrogram. The micrograph shows a part of two adjacent cells; mf = myofilaments; N = nucleus; m = mitochondria; es = extracellular space. Final magnification = 20,000 \times . The inset shows, at higher magnification (60,000 \times), two small gap junctions (n) in the zone of close apposition of the two cells.

found at all levels between the nodal cell group and the myocardial cells of the crista terminalis. On the crista terminalis, the nodal fibers changed direction and were seen in longitudinal section, spreading in a lateral direction. Here, no distinct border could be detected between atrial and nodal cells. Ultrastructurally, there was a gradual transition in cell type toward the periphery from that observed in the pacemaker area to an atrial working myocardium cell. The shape and arrangement of the cells became more regular and the myofilaments became more numerous and better organized. All types of specialized junctions were observed more frequently, particularly the gap junctions, which also became larger in size. An example of the ultrastructure of these cells is given in Figure 6. No preferential location of the gap junctions was observed. Regarding the configuration of the action potentials recorded in this zone, we observed a gradual transition from a pacemaker type to an atrial type also (Fig. 7): the slope of diastolic depolarization became less steep, and amplitude and V_{max} increased (see also Fig. 2).

Blocking of the conduction toward the septal side of the preparation occurred at the septal fringe of the sinus node. This is about half way between the crista terminalis and the left branch of the sinoatrial

ring bundle. Here the nodal cell group bordered on the atrial fibers, whereas a zone of transition was very small or nearly absent (see Fig. 1c). No anatomical obstacle, such as partitions of connective tissue, could be discovered; at all levels there was continuity in cardiac tissue. Figure 8 shows the double-component action potentials which were recorded in the zone of block. It can be seen that the first component of these action potentials closely followed the action potential at the pacemaker side, whereas the second was nearly synchronous with that at the septal side. The width of this zone of double-component action potentials varied in different preparations from 0.2 to more than 1 mm; double-component action potentials were observed as well in the nodal as in the atrial tissue. We took several samples from this area for electron microscope investigation, and preliminary results showed that gap junctions occurred here with about the same frequency as in the pacemaker area.

Discussion

Suitability of the Method

Our method of mapping the electrical activity by means of multiple impalements with one microelectrode is based on the assumption that during an

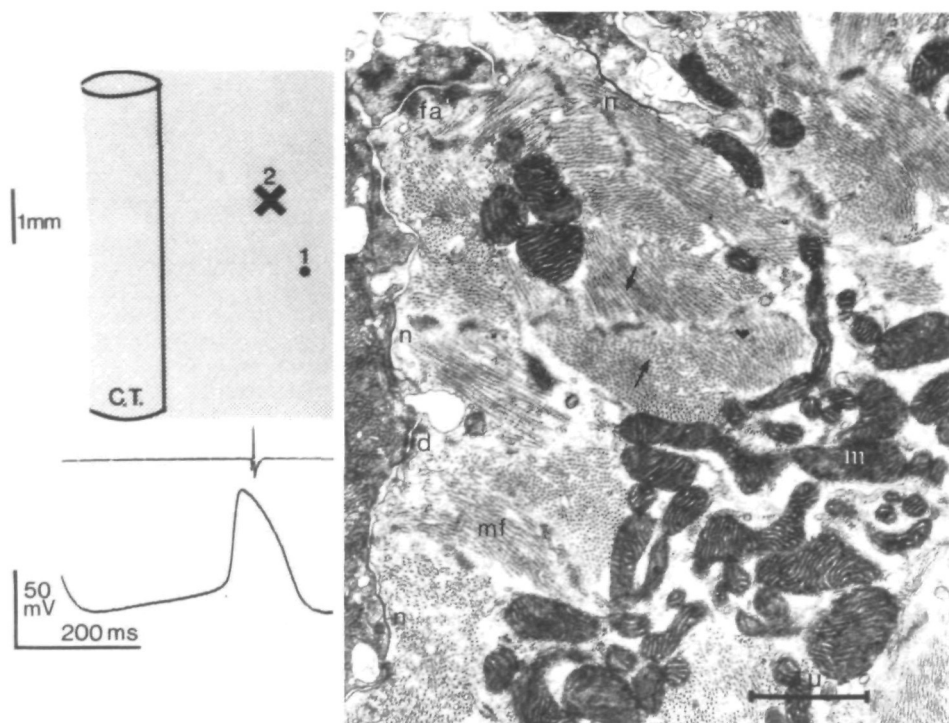


FIGURE 6 Ultrastructure of latent pacemaker cells selected from the preferential route of conduction in the same preparation as was used for Figure 5. The scheme on the left shows the location of these cells (site 2) with respect to the crista terminalis and the cells shown in Figure 5 (site 1). The action potential underneath shows that these cells had a slower diastolic depolarization and a faster phase 0 depolarization and that they were activated later in the cardiac cycle. The micrograph shows that more myofilaments (mf) are present than in the cells of site 1, but that the contractile system is still not well organized. Myofibrils are present side by side, both in cross and longitudinal sections (arrows). A small desmosome (d), a fascia adherens (fa), and three gap junctions are present in the zone of close apposition of the two cells. Final magnification = 20,000 \times .

experiment every excitation of the sinus node has the same origin and propagation. In view of the regular beat-to-beat interval (differences between consecutive intervals were less than 2 msec), which increased only slightly during an experiment (10–15 msec/hour), the process of excitation seemed indeed to be a stable one. To check this, we did some controls. During long impalement of one cell (more than one-half hour), the time to reference of the recorded action potential remained constant within 1 msec. Repeated impalements at the same site resulted in reproducible shape and timing of the action potential, even after some hours. Here it must be mentioned that the accuracy of determination of the site of impalement was limited by the movements of the contracting preparation, which, however, never exceeded 0.05 mm. We suppose that the preparation remained in such a stable condition because the thinness of the tissue at the level of the sinus node (0.1–0.3 mm) allowed a good diffusion between extracellular space and bathing fluid. Within the sinus node the ultrastructure of the cells showed no signs of necrosis, whereas in the center of the much thicker crista terminalis necrotic cells commonly were found. The activation pattern of

the sinus node is represented in two dimensions. In the intercaval region, this seemed to be justified, because action potentials recorded at different depths were synchronous and identical. In the crista terminalis, however, we observed different activity at different depths (see also Masuda and Paes de Carvalho, 1975). Here only recordings from superficial cells were used.

Dominant Pacemaker Site

Several criteria for defining the dominant pacemaker site have been compared. It appeared clearly that the configuration of the action potential as the only criterion does not identify the dominant pacemaker site, as can be seen for example in Figure 8. In this preparation, the action potential recorded at site D showed the characteristics of a dominant pacemaker action potential (steep diastolic depolarization and gradual transition into phase 0 depolarization), but regarding its timing in relation to the other action potentials, site D cannot be regarded as the dominant pacemaker site. Likewise, a low rate of phase 0 depolarization seems to be a rather nonspecific feature, which is present in all cells in the compact portion of the node (Fig. 4).

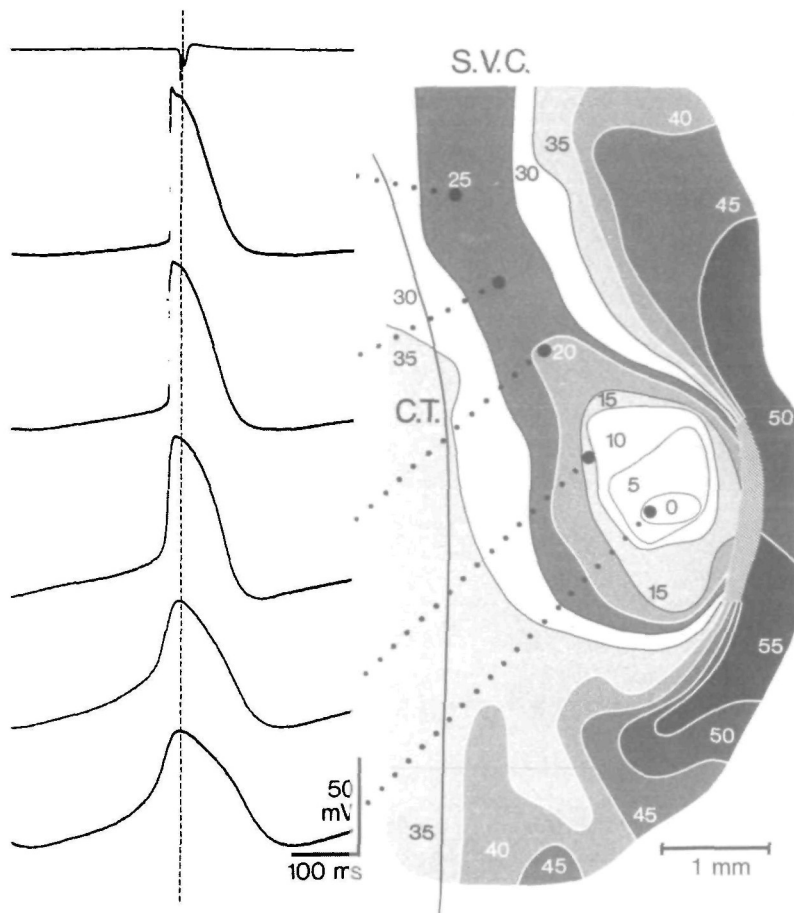


FIGURE 7 Configuration of action potentials recorded in the route of preferential conduction. The dashed line indicates the time reference. Toward the periphery, action potentials show an increase in amplitude and V_{max} and a decrease in rate of diastolic depolarization. The numbers in the map give the activation time in milliseconds. The area in which two component action potentials were recorded is hatched in the activation map.

Determination of the activation order within the node gave great problems because the excitation threshold cannot be determined from simple V_t tracings. Sano and Yamagishi (1965) chose the moment of \dot{V}_{max} as an approximation of the activation moment. However, it generally is accepted that the excitation threshold lies well below the voltage where \dot{V}_{max} is observed. For the cells in the central part of the node, this easily can mean an error of more than 10 milliseconds. Because this error is not the same for the surrounding latent pacemaker cells in which the upstroke lasts only a few milliseconds, this method of timing will introduce an artifact in the activation map of the central part of the node. For this reason, we chose V_{hfamp} as an approximation of the excitation threshold, a point in the action potential that precedes the moment of \dot{V}_{max} in the cells with a steep diastolic depolarization. Cells that reached V_{hfamp} earliest appeared to have the steepest diastolic depolarization (Fig. 4). So, the timing of V_{hfamp} might be useful for locating the dominant pacemaker.

Some authors demonstrated that, in the center of the sinus node, the fast inward current system is inactivated or not present, whereas in the surrounding latent pacemaker cells, which have a more neg-

ative maximal diastolic potential, some fast-channel activity is present (Yamagishi and Sano, 1966; Kreitner, 1975; Kohlhardt, 1976; Noma et al., 1978). Therefore, it is conceivable that the pacemaking cells activate their neighboring cells during the accelerating diastolic depolarization, without activating a separate current for their own systolic depolarization.

Therefore, we preferred the rate of depolarization at the end of diastole as criterion for exact definition of the dominant pacemaker. The highest rates were observed in a rather large, not sharply delineated area (about 0.3 mm^2), situated within the compact portion of the node. Centrally in this area, we observed completely identical and synchronous electrical activity in a group of cells covering an area of about 0.1 mm^2 only. We roughly estimated that this group consists of about 5000 cells. This observation of synchronous activity fits with the model that pacemaker cells behave as a large group of electrically coupled oscillators (Winfree, 1967; Torre, 1976). In view of this model, we can see the central group of at least 5000 cells as the leading cell group, of which, however, the oscillatory behavior will be influenced also by the surrounding cells, which tend to oscillate at a lower frequency. There-

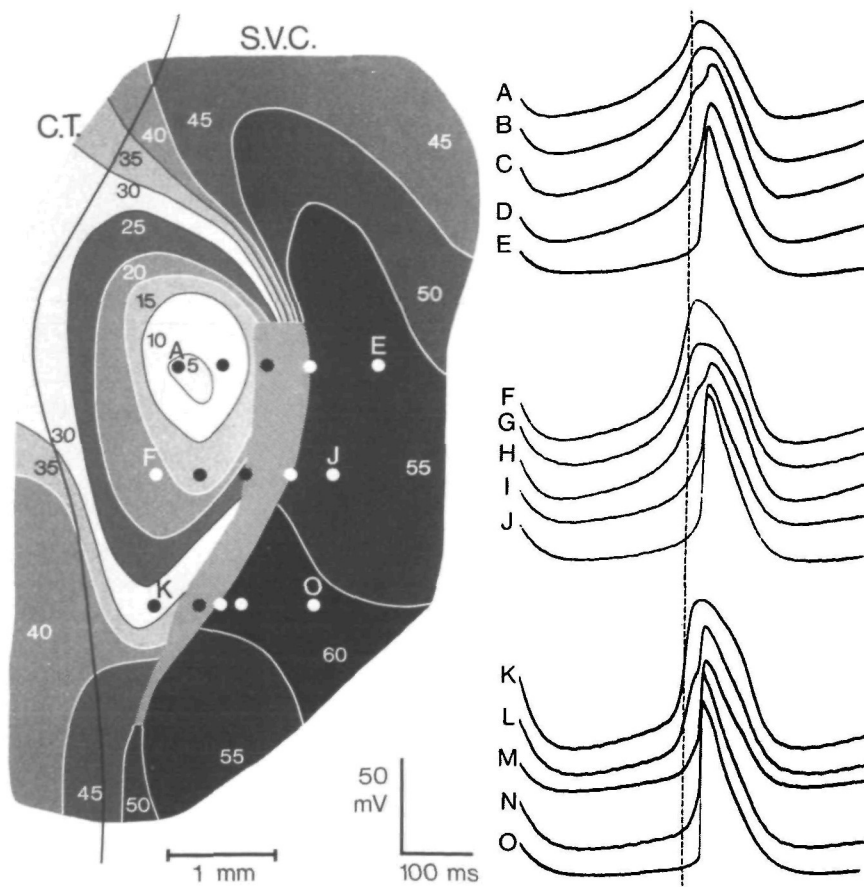


FIGURE 8 Conduction block in the sinus node. The action potentials (on the right side) were recorded at corresponding points of the activation map (on the left side). The dashed line indicates the time reference. The area in which two components in the action potential were clearly visible is hatched in the activation map.

fore, sharp delimitation of the leading pacemaker will be impossible.

For electrical coupling, we found a morphological substrate in the presence of gap junctions. Whereas other authors stressed their absence in the sinus node (James et al., 1966; Ayettey and Navaratnam, 1978), we found them as a common finding. At least one gap junction was present along every cell contour as seen in ultrathin sections. We suppose that this difference in result is merely a consequence of a different fixation procedure. The staining with uranyl acetate results in a better visibility of gap junctions. We roughly estimated that every cell in the pacemaker center is coupled with at least 100 gap junctions to the neighboring cells. Random sectioning (50 nm thickness) of these cells (8 μm in diameter, 25–30 μm long) will result in 150–400 sections; according to its extent, every gap junction will be present in one or two sections. From such an estimation, it is not possible to predict the magnitude of coupling, but the fact that gap junctions are smaller and less numerous than between atrial cells fits with the model of Torre (1976) that for synchronization weak coupling is sufficient.

Regarding the position of the leading pacemaker cells within the node, it must be noted that this

study concerns the function of the node under standard conditions. It is, however, known from the literature that there are several interventions which can induce a shift of the dominant pacemaker site within the node (Brooks and Lu, 1972; West, 1955; Bouman et al., 1968; Bouman et al., 1978).

Conduction within the Sinus Node

From the data of our activation maps, it is not possible to calculate accurately the conduction velocity in the central portion of the node, where the action potentials show different upstroke velocities (see discussion above). The conduction velocity will be overestimated and is thus lower than the calculated 2–8 cm/sec. For conduction toward the periphery, we did not find any well-defined specialized conduction pathways in our histological reconstruction, as described by James (1967) or Sano and Iida (1968). The activation maps showed that spread of excitation occurred in all directions except that of the interatrial septum, which is in accordance with the results of Sano and Yamagishi (1965). The preferential route of conduction can be explained by the orientation of the cells that are arranged in parallel. If one assumes that gap junctions make a major contribution to the intracellular resistance of

the syncytium, a lower resistance is expected along the long axis of the cells as there are fewer gap junctions per unit of distance in this direction. This agrees with results of Bukauskas et al. (1977), who found in the sinus node region a longer length constant in the axial direction than in the transverse direction. This explains adequately the higher velocity of conduction in the axial direction. The increasing speed of conduction toward the periphery coincided with an increase in V_{max} and amplitude of the action potentials and with an increase in number of the gap junctions. Although the action potentials resemble those recorded from perinodal fibers described by Strauss and Bigger (1972), we did not find that these cells "served as the site of normal conduction delay for impulses leaving the sinus node" as postulated by these authors; on the contrary, conduction velocity increased markedly, especially along the long axis of the cells when the front left the compact portion and moved toward the crista terminalis. An intriguing question is the block of conduction toward the septal side. No morphological basis was found in the histological reconstruction, such as, for example, a zone of connective tissue, and there was no lack of cell coupling (supposing that the morphologically identified gap junctions are functionally intact). The small efficacy of the excitation wave from the nodal side appears not to be the cause of block; an excitation wave from the septal side is blocked as well, as was demonstrated by Sano and Yamagishi (1965). In the blocking fringe, we recorded action potentials with double components such as can be found in other cardiac tissues with slow conduction. Van Capelle and Janse (1976) gave arguments for the concept that double-component action potentials are associated with a zone of reduced excitability and that the components are a result of electrical interaction with neighboring cells rather than of activation of local membrane currents. Our observations fit with this concept. Figure 8 shows that the first and second components closely follow the electrical activity on, respectively, nodal and septal side. So we conclude that reduced excitability of the cells leads to conduction block of the sinus node impulse toward the septal side.

Acknowledgments

We are most grateful to C.E. Besselsen and M.J. Klaver for unfailing technical assistance, to A.A. Meijer and A.W. Schreurs for valuable technical advice, and to A. van Gent for writing excellent computer programs. We are also grateful to Dr. M.A. Allessie, Dr. F.I.M. Bonke, Dr. H.J. Jongsma, and Dr. M.J. Janse for helpful discussions.

References

- Ayette AS, Navaratnam, V (1978) The T-tubule system in the specialized and general myocardium of the rat. *J Anat* **127**: 125-140
- Bonke FIM (1973) Electrotonic spread in the sinoatrial node of the rabbit heart. *Pfluegers Arch* **339**: 17-23
- Bouman LN, Gerlings ED, Biersteker PA, Bonke FIM (1968) Pacemaker shift in the sino-atrial node during vagal stimulation. *Pfluegers Arch* **302**: 255-267
- Bouman LN, Mackay AJC, Bleeker WK, Becker AE (1978) Pacemaker shifts in the sinus node: Effects of vagal stimulation, temperature, and reduction of extracellular calcium. In *The Sinus Node*, edited by FIM Bonke. The Hague/Boston/London, Martinus Nijhoff, pp 245-258
- Brooks CMcC, Lu HH (1972) The sinoatrial pacemaker of the heart. Springfield, Ill., Charles C Thomas
- Bukauskas FF, Veteikis RP, Gutman AM, Mutskus KS (1977) Intracellular coupling in the sinus node of the rabbit heart. *Biofizika* **22**: 108-112
- Glauert AM, Glauert RH (1958) Araldite as embedding medium for electron microscopy. *J Biophys Biochem Cytol* **4**: 191-194
- James TN (1967) Anatomy of the cardiac conduction system in the rabbit. *Circ Res* **20**: 638-648
- James TN, Sherf L, Fine G, Morales AR (1966) Comparative ultrastructure of the sinus node in man and dog. *Circulation* **24**: 139-163
- Karnowsky MJ (1967) The ultrastructural basis of capillary permeability studied with peroxidase as tracer. *J Cell Biol* **35**: 213-221
- Kohlhardt M, Figulla HR, Tripathi O: (1976) The slow membrane channel as the predominant mediator of the excitation process of the sinoatrial pacemaker cell. *Basic Res Cardiol* **71**: 17-26
- Kreitner D (1975) Evidence for the existence of a rapid sodium channel in the membrane of rabbit sinoatrial node cells. *J Mol Cell Cardiol* **7**: 655-662
- Lawson WH (1936) Elastic tissue staining; modification of Weigert-Sheridan method. *J Tech Meth* **16**: 42-52
- Lee BB, Mandl G, Stean JPB (1969) Microelectrode tip position marking in nervous tissue: A new dye method. *Electroencephalogr Clin Neurophysiol* **27**: 610-613
- Masuda MO, Paes de Carvalho A (1975) Sinoatrial transmission and atrial invasion during normal rhythm in the rabbit heart. *Circ Res* **37**: 414-421
- McEwen LM (1956) The effect on the isolated rabbit heart of vagal stimulation and its modification by cocaine, hexamethonium and ouabain. *J Physiol (Lond)* **131**: 678-689
- Noma A, Yanagihara K, Irisawa I (1978) Ionic currents in rabbit sinoatrial node cells. In *The Sinus Node*, edited by FIM Bonke. The Hague/Boston/London, Martinus Nijhoff, pp 301-310
- Paes de Carvalho A (1961) Cellular electrophysiology of the atrial specialized tissues. In *The Specialized Tissues of the Heart*, edited by A Paes de Carvalho, WC de Mello, BF Hoffman. New York, Elsevier, pp 115-133
- Pollack GH (1977) Cardiac pacemaking: An obligatory role of a catecholamines? *Science* **196**: 731-738
- Reynolds ES (1963) The use of lead citrate at high pH as an electron opaque stain in electron microscopy. *J Cell Biol* **17**: 208-212
- Sano T, Iida Y (1968) The sinoatrial connection and wandering pacemaker. *J Electrocardiol* **1**: 147-154
- Sano T, Yamagishi S (1965) Spread of excitation from the sinus node. *Circ Res* **16**: 423-430
- Schreurs AW, Meijer AA, Bouman LN, Bonke FIM (1974) Micromanipulator with an electrode driver used for microelectrode work. *Pfluegers Arch* **346**: 163-166
- Seyama I (1976) Characteristics of the rectifying properties of the sino-atrial node cell of the rabbit. *J Physiol (Lond)* **255**: 379-397
- Strauss HC, Bigger JT (1972) Electrophysiological properties of the rabbit sinoatrial perinodal fibers. *Circ Res* **31**: 490-505
- Torre V (1976) A theory of synchronization of the heart pacemaker cells. *J Theor Biol* **61**: 55-71
- Tranum-Jensen J (1976) The fine structure of the atrial and atrioventricular (AV) junctional specialized tissues of the rabbit heart. In *The Conduction System of the Heart*, edited by HJJ Wellens, KI Lie, MJ Janse. Leiden, Stenfert Kroese B.V., pp 55-81
- Trautwein W, Uchizono K (1963) Electron microscopic and

- electrophysiologic study of the pacemaker in the sinoatrial node of the rabbit heart. *Z Zellforsch Mikrosk Anat* 61: 96-109.
- Truex RC (1976) The sinoatrial node and its connections with the atrial tissues. In *The Conduction System of the Heart*, edited by HJJ Wellens, KI Lie, MJ Janse. Leiden, Stenfert Kroese B.V., 209-227.
- Van Capelle FJL, Janse MJ (1976) Influence of geometry on the shape of the propagated action potential. In *The Conduction System of the Heart*, edited by HJJ Wellens, KI Lie, MJ Janse. Leiden, Stenfert Kroese B.V., pp 316-336.
- West TC (1955) Ultramicroelectrode recording from the cardiac pacemaker. *J Pharmacol Exp Ther* 115: 283-290.
- Winfree AT (1967) Biological rhythms and the behavior of populations of coupled oscillators. *J Theor Biol* 16: 15-42.
- Yamagishi S, Sano T (1966) Effect of tetrodotoxin on the pacemaker action potential of the sinus node. *Proc Jpn Acad* 42: 1194-1196.

Asymmetry of Consequences of Drug Disposition Mechanisms in the Wall of the Rabbit Aorta

RODOLFO PASCUAL AND JOHN A. BEVAN

SUMMARY The contraction elicited by norepinephrine (NE) and histamine (H) in the rabbit aortic strip occurs after a shorter latency and increases at a higher initial velocity to a greater steady state level when drug entry is limited to the intimal compared with the adventitial surface. Differences in the steady state contraction, but not in latency or initial velocity, disappear when intramural disposition pathways of the two agonists are blocked pharmacologically by deoxycorticosterone and a combination of iproniazid and 17- β -estradiol, respectively. These and other observations are consistent with the hypothesis that inner vascular smooth muscle cells respond more than outer cells to submaximal concentrations of NE and H, an explanation that accounts for the persistence of differences in latency and initial velocity of response after disposition blockade. Although the effectiveness of disposition mechanisms in reducing agonist concentration may be uniform through the aortic medial thickness, because of differences in muscle sensitivity, the consequence of disposition on the contractile response to agonists entering through the adventitia would be greater than that through the intima. Thus, disposition mechanisms in the outer smooth muscle lamellae provide a functional barrier to susceptible agonists entering through the outside vessel wall surface. *Circ Res* 46: 22-28, 1980

The characteristics of the steady state contractile response of rabbit thoracic aortic strips to norepinephrine (NE) and to histamine (H) vary according to whether these drugs enter the media via the adventitia or the intima (Pascual and Bevan, 1978). Differences in the case of NE persist after the process of amine uptake into the neuronal plexus is blocked pharmacologically. They are not due to the presence of the tunica adventitia on the outer surface of the media in that the difference in response characteristics persists after physical removal of the adventitia (Pascual and Bevan, 1979). Furthermore, there is evidence that the adventitia does not constitute a significant barrier to the diffusion of NE

(Bevan and Torok, 1970). This conclusion also is supported by the demonstration that 10 times as much NE and its metabolites overflow via the adventitia than via the intima on stimulation of the neuronal plexus, which is located between the tunica adventitia and the tunica media of the pulmonary artery. This vessel, like the aorta, is an elastic artery (Bevan and Su, 1974). The pattern of response of the strip to intimal entry of drug is essentially the same as that of the intact strip.

The difference in response to intimal compared to adventitial drug entry could be due to nonuniformity of muscle characteristics in the tunica media such as smooth muscle cell agonist sensitivity and contractility, cell density, or intramural drug disposition mechanisms. Differences in vascular smooth muscle sensitivity as a function of depth in the blood vessel wall have been described in the sheep carotid artery—the inner layer being more sensitive to NE and H than the outer (Graham and Keatinge, 1972). Extraneuronal uptake and metabolism are important in the disposition of NE by the rabbit thoracic aorta and influence the contractile response of the tissue (Kalsner and Nickerson, 1969;

From the Department of Pharmacology, School of Medicine and Brain Research Institute, University of California Center for Health Sciences, Los Angeles, California.

Supported by U.S. Public Health Service Grant HL 20581 and the Del Amo Foundation.

Dr. Pascual was visiting from the Department of Pharmacology and Therapeutics, University of Autonoma, Madrid, Spain.

Address for reprints: John A. Bevan, M.D., Department of Pharmacology, School of Medicine, University of California, Los Angeles, California 90024.

Received November 3, 1978; accepted for publication September 12, 1979.